

University of South Australia

The Library
www.library.unisa.edu.au

Educating Professionals, Creating and Applying Knowledge, Engaging our Communities

NOTICE: this is the accepted author manuscript (AAM) or post-print which was accepted for publication in *Bone.* Changes resulting from the publishing process, such as peer review, editing, corrections, structural formatting, and other quality control mechanisms are reflected in this document. This version is licensed under a Creative Commons CC-BY-NC-ND 4.0 license (http://creativecommons.org/licenses/by-nc-nd/4.0/).

A definitive version was subsequently published in *Bone,* vol. 93, pp. 22-32, 2016, DOI: dx.doi.org/10.1016/j.bone.2016.09.008

Pulsed electromagnetic fields stimulate osteogenic differentiation and maturation of osteoblasts by upregulating the expression of BMPRII localized at the base of primary cilium

Yan-Fang Xie [a,1] , Wen-Gui Shi [b,1] , Jian Zhou [a], Yu-Hai Gao [a], Shao-Feng Li [a], Qing-Qing Fang [a], Ming-Gang Wang [c], Hui-Ping Ma [d], Ju-Fang Wang [b], Cory J Xian [e], Ke-Ming Chen [a*]

[a] Institute of Orthopaedics, Lanzhou General Hospital, Lanzhou Command of CPLA, Lanzhou 730050, People's Republic of China; [b] Gansu Key laboratory of Space Radiobiology, Institute of Modern Physics, Chinese Academy of Sciences, Lanzhou 730000, P.R China; [c] School of life science and engineering, Lanzhou University of Technology, Lanzhou 730050, People's Republic of China; [d] Department of Pharmacy, Lanzhou General Hospital, Lanzhou Command of CPLA, Lanzhou 730050, People's Republic of China; [e] Sansom Institute for Health Research, School of Pharmacy and Medical Sciences, University of South Australia, Adelaide, SA 5001, Australia

Email Address:

xieyanfang@lut.cn, shiwengui@impcas.ac.cn, zhouj12@lzu.edu.cn, guyansuo@gsau.edu.cn, leesf@st.gsau.edu.cn, 132085238002@lut.cn, mgwang@lut.cn, mahuiping2014@gszy.edu.cn, jufangwang@impcas.ac.cn, cory.xian@unisa.edu.au, chenkm@lut.cn

Running Title: PEMFs increase BMPRII expression at ciliary base

Word Counts/ Character: Abstract=215/1,331; Manuscript= 4954/28,792

Number of Figures: 8

Funding Sources: National Natural Sciences Foundation of China (No. 81270963, 81471090 to KMC, and 81571847 to HPM); International Science & Technology Cooperation Program of China (No. 2015DFR30940 to KMC and JFW)

***Correspondence:**

Institute of Orthopaedics, Lanzhou General Hospital, Lanzhou 730050, China Phone: (+86) 0931 8994327; E-mail address: chenkm@lut.cn

Conflict of interest: All authors have no conflicts of interest.

[1] These authors contributed to this work equally

Abstract

Pulsed electromagnetic fields (PEMFs) have been considered as a potential candidate for the prevention and treatment of osteoporosis, however, the mechanism of its action is still elusive. We have previously reported that 50 Hz 0.6mT PEMFs stimulate osteoblastic differentiation and mineralization in a primary cilium- dependent manner, but did not know the reason. In the current study, we found that the PEMFs promoted osteogenic differentiation and maturation of rat calvarial osteoblasts (ROBs) by activating bone morphogenetic protein BMP-Smad1/5/8 signaling on the condition that primary cilia were normal. Further studies revealed that BMPRII, the primary binding receptor of BMP ligand, was readily and strongly upregulated by PEMF treatment and localized at the bases of primary cilia. Abrogation of primary cilia with small interfering RNA sequence targeting IFT88 abolished the PEMF-induced upregulation of BMPRII and its ciliary localization. Knockdown of BMPRII expression level with RNA interference had no effects on primary cilia but significantly decreased the promoting effect of PEMFs on osteoblastic differentiation and maturation. These results indicated that PEMFs stimulate osteogenic differentiation and maturation of osteoblast by primary cilium-mediated upregulation of BMPRII expression and subsequently activation of BMP-Smad1/5/8 signaling, and that BMPRII is the key component linking primary cilium and BMP-Smad1/5/8 pathway. This study has thus revealed the molecular mechanism for the osteogenic effect of PEMFs.

Keywords Pulsed electromagnetic fields, Osteoblasts, Primary cilia, BMP-Smad1/5/8 signaling, BMPRII

Introduction

Osteoporosis is a significant public health problem that is widely undertreated, despite the availability of many options of treatment. As some treatments are defective, ineffective, expensive, low in patient compliance, and/or risky (as they disturb normal bone turnover physiology and/or cause significant side effects or even cancer), searching for alternative and effective therapies for osteoporosis is necessary and has been drawing attention of many clinicians and researchers [1,2]. While electromagnetic fields (EMFs) of extremely low frequency have been considered as a promising therapy for a wide range of bone diseases, such as fresh and nonunion fractures and osteoarthritis [3], accumulating evidence has now shown that pulsed electromagnetic fields (PEMFs) as an alternative noninvasive method were capable of producing satisfying therapeutic effects on osteoporosis [4]. PEMFs promote osteogenesis and mineralization of bone cells and prevent bone loss in animal models of disuse or tail-suspension osteoporosis and ovariectomy-induced bone loss [5,6]. Clinical investigations further confirmed that PEMFs increased bone mineral density and prevented bone loss in osteoporosis patients [7,8]. However, the action mechanism of PEMFs in preventing bone loss is still elusive.

We previously reported that waveforms, frequencies, intensities, and exposure duration influenced effects of EMFs on osteogenesis and the best therapeutic effects of EMFs could be obtained by defining their optimal application parameters. 50 Hz sinusoidal EMFs were found to promote the differentiation and mineralization potentials of osteoblasts in an intensity-dependent manner with peak activity shown at 1.8 mT and 3.6 mT [9,10]. We recently further reported that 0.6 mT was the optimal intensity of 50 Hz PEMFs from the 0.6 mT to 3.6 mT range in stimulating both proliferation and osteogenic differentiation of rat calvarial osteoblasts *in vitro*[11]. In addition, we also demonstrated that the osteogenic effect of PEMFs needs the existence, on the osteoblasts, of a primary cilium, which is a solitary, immotile, microtubule-based organelle growing from the centrosome and projecting from the vertebrate cell surface [11,12]. However, the detailed mechanism of primary cilium in mediating the osteogenic effect of PEMFs is not clear.

Primary cilium has been demonstrated to play an important mechanosensory role in numerous tissues. More and more evidence suggests that primary cilia might mediate sensing of mechanical stresses that occur with skeletal development [13,14]. When primary cilia were abrogated in MC3T3-E1 osteoblasts, the osteogenic responses to fluid flow were attenuated [15]. The upregulation of osteogenic factors in MLO-Y4 osteocytes normally experienced in response to fluid flow was abolished when

ciliogenesis was inhibited [16]. The mice with an osteoblast- and osteocyte-specific knockout of Kif3a, a gene essential to primary cilia formation and function, exhibited diminished bone formation in response to loading [17]. These results indicate that primary cilia are mechanosensors in bone cells; however, the molecular basis of mechanotransduction has not been fully elucidated.

As a key coordinator of signal pathways like receptor tyrosine kinases (RTKs), platelet-derived growth factor receptor (PDGFR), Hedgehog (Hh), Wingless/Int-1 (Wnt), neuronal and purinergic receptors [18-22], there is a variety of receptors, ion channels and transporter proteins present in the primary cilia, and some downstream effectors of these pathways were localized to the cilium [23,24]. Recently, more new primary cilium-located proteins were reported, including G protein-coupled receptors, anoctamin and septin, which further confirmed the role of primary cilium as a key coordinator of signaling pathway [25-27]. In particular, transforming growth factor (TGF-β) receptors have been reported to be localized to the ciliary tip and base in fibroblasts, and TGF-β stimulation increases receptor localization and activation of SMAD2/3 at the ciliary base. When primary cilia were abrogated, TGF-β signaling in fibroblasts was reduced, which demonstrates that primary cilia play an indispensable role in TGF-β signaling [28].

Bone morphogenetic proteins (BMPs), belonging to the large TGF-β super family, have diverse functions in embryonic development and have been demonstrated to play crucial roles in osteogenesis [29]. Among BMP family members, BMP2 has been extensively studied for its variety of functions, particularly in embryonic skeletal development and postnatal bone remodeling and bone repair [30,31]. A recent human genetic study indicated that polymorphisms of BMP2 expression are linked to a high risk for osteoporosis [32]. BMP-Smad1/5/8 signaling is a canonical osteogenesis-related pathway, which is critical for osteogenic differentiation [33]. There are two subtypes of BMP receptors, BMPR-I and BMPR-II, which are serine-threonine kinase receptors. BMPRII is the primary binding site for BMP ligand. Upon BMP binding to BMPRII, BMPRI is phosphorylated and activated, and the activated BMPRI in turn phosphorylates the intracellular BMP effector proteins, Smad proteins 1, 5 and 8 (Smad1/5/8). Phosphorylated Smads1/5/8 forms a complex with Smad4 and translocates to the nucleus, whereby it regulates the transcription of bone-specific genes [34-36].

Here we hypothesized that PEMFs stimulate the osteoblastic differentiation by activating BMP-smad1/5/8 pathway, some components of this pathway are associated with primary cilia, and that lack of primary cilia or their abnormal status could affect these components and therefore disturb the signal

transduction of BMP pathway, which consequently impact the osteogenic effect of PEMFs. In this study, we firstly examined whether BMP-smad1/5/8 pathway was involved in the PEMFs-induced osteogenic differentiation, then we investigated whether primary cilia was indispensable for the activation of the pathway. Lastly, the connection between the primary cilia and BMP-smad1/5/8 pathway was explored by examining co-localization of cilia with the signaling proteins. Our results verified our hypothesis and indicated that BMPRII is the linking protein between primary cilia and the BMP-smad1/5/8 pathway that underlies the osteogenic effect of PEMFs.

Materials and Methods

Reagents

Dulbecco's modified Eagle's medium (DMEM) was obtained from Gibco (Gibco, Gaithersburg, MD, USA). Fetal bovine serum (FBS), collagenase II and trypsin were purchased from Gibco BRL (Gaithersburg, MD, USA). β-glycerophosphate, dexamethasone, and ASAP (ascorbic acid 2-phosphate) were all from Sigma (St. Louis, MO, USA). BMP2 was the product of Abcam (recombinant full length human protein, ab50099, Abcam, Cambridge, MA). All other chemicals were of analytical grade.

Animals and PEMFs device

Newborn Wistar rats were obtained from the Animal Breeding Center of Gansu University of Traditional Chinese Medicine (Lanzhou, China). Animal experiments were approved by Animal Ethics Committee of Lanzhou General Hospital and were conducted according to NIH Guidelines for the Care and Use of Laboratory Animals. The device producing EMFs was self-made (Patent No.ZL 20112 0528654.3) as previously reported by Yan et al [11]. The cells to be treated were cultured in 60-mm culture dishes (Nunc, Roskilde, Denmark) and the dishes were placed in the area with good uniformity within the specially designed coils, which ensures all cells are subjected to the same electromagnetic fields. To avoid the unwanted effect of heat produced by the device, a digital temperature sensor (Model DS18B20, EVERY, Beijing, China) was installed in the solenoid. When the solenoid's temperature exceeds 37.5 °C, the sensor would give warning signals. PEMFs of 50Hz frequency, 0.6mT intensity and 50% duty ratio, produced by this device, were used in this experiment.

Isolation and culture of rat calvarial osteoblasts

The rat calvarial osteoblasts (ROBs) were isolated and pooled from 10 neonatal rats as previously described [37]. The skull bone were obtained aseptically and cleaned of adhering soft tissues, rinsed by sterile phosphate buffered saline (PBS pH 7.4) and minced to small pieces. The bone pieces were digested at 37 °C with 0.5 mg/ml trypsin (twice, 10 min each), and then 1 mg/ml collagenase II (six times, 20 min each). The released cells from the last four collagenase digestions were pooled and filtered through a 200-μm sieve to remove bone debris. The collected cells were suspended in DMEM plus 10% heat-inactivated FBS, 100 U/ml penicillin and 1000 U/ml streptomycin, and cultured in 100-mm culture dishes in a humidified atmosphere of 5% CO_2 at 37 °C. When the cells reached 70-80% confluence, they were subcultured in 60-mm dishes at 2×10^4 cells/ml and used for assays described below. The cells were treated by PEMFs from 5 min to 120 min to observe the early or short term effect of PEMFs. For examining the long term effect of PEMF treatments, the cells were cultured in the osteogenic culture medium (containing 10 mM β-glycerophosphate and 0.1 mM L-ascorbic acid-2- phosphate) and treated by PEMFs at 60 min/day for up to 12 days. For immunostaining experiments, the cells were grown on 76×48×1-mm UV-transparent quartz slides (Fisher Scientific, Waltham, MA).

Alkaline phosphatase (ALP) activity measurement and calcified nodule assay

After 3 days and 6 days of PEMF treatment at 60 min/day, the ALP activities were measured biochemically with a modified method of King using a commercial kit as instructed (Nanjing Jiancheng Bioengineering Ltd, Nanjing, China). The result was expressed as nmol phenol/15 min/mg protein. The calcified nodules formed after 12 days were assayed by alizarin red staining. The cells were fixed for 10 min by 10% formaldehyde and stained by 0.1% alizarin red for 1h at 37°C. The total number and area of red nodules were measured by Image-Pro Plus 6.0 software.

Immunofluorescence staining and confocal microscopy

ROBs grown on coverslips were washed by PBS 3 times and fixed in 4% paraformaldehyde and permeabilized with 0.2% Triton X-100 (PBST) for 10 min. The coverslips were blocked with 5% bovine serum albumin (BSA) in PBS for 30min. Immunostaining was carried out using primary antibodies targeted against rabbit anti-phospho-Smad1/5/8 (1:400), mouse anti-acetylated α-tublin (1:200), rabbit anti-BMPRII (1:500), rabbit anti-BMPRIA (1:200) and rabbit anti-BMPRIB (1:500; all above antibodies from Abcam). The secondary antibodies were rhodamine-labeled goat anti-rabbit IgG (1:500) and FITC-

labeled goat anti-mouse IgG (1:500; both from KPL, Gaithersburg, MD). The staining results were imaged on a laser-scanning confocal microscope (Nikon C-1; Nikon, Tokyo, Japan) using a 1.4 NA×60 UV-corrected objective. The relative intensities were measured using Image-Pro Plus 6.0 software.

RNA interference of IFT88 and BMPRII

To prevent cilium formation, ROBs were treated with a siRNA to knockdown the expression of intraflagellar transport 88 homolog (IFT88), a protein required for formation and assembly of cillia [38-40]. Oligo nucleotides of siRNA targeting IFT88 (sequence:5´-GGAUAUGGGUC CAAGACAUCC-3´) and a corresponding negative control siRNA were synthesized and cloned into the pENTRTM/U6 vectors (Genechem, Shanghai, China) and transfected into ROBs using lipofectamine 2000 (Invitrogen, Carlsbad, CA). Green fluorescent protein (GFP) was used as an indicator for success of transfection. Assays for evaluating gene silencing efficiency were performed 24h after transfection by RT-PCR and Western blotting. For BMPRII silencing, one siRNA targeting BMPRII (sequence: 5´-GCAGAAATGTCCTGGTAAA-3´) and a corresponding negative control siRNA (Invitrogen) were used. The assays for checking BMPRII silencing efficiency were carried out similarly as for IFT88 interference.

Western blotting

The protein expression levels of BMP2, p-Smad1/5/8, Smad1/5/8, BMPRIA, BMPRIB, BMPRII and other osteogenesis markers (COL-1, Runx-2 and Osx) were examined by Western blotting. Briefly, cells were lysed and homogenized in RIPA lysis buffer (Santa Cruz Biotech, Dallas, Texas). The supernatant was obtained by centrifugation at 4°C for 30 min at 12,000 rpm and the protein content was quantified by a BCA kit (Thermo Fisher Scientific, Waltham, MA). The samples were separated by 12% SDS-PAGE (Solarbio, Beijing, China), transferred onto PVDF membranes, and probed with rabbit anti-Smad1/5/8 (1:1000) and anti-p-Smad1/5/8 (1:1000, both from Cell Signaling, Danvers, MA), rabbit anti-BMPRII (1:800, Abcam), rabbit anti-BMP2 (1:800, Abcam), rabbit anti-COL-1 (1:1000, Santa Cruz Biotech), rabbit anti-Runx-2 (1:1000, Abcam), rabbit anti-Osx (1:1000, Abcam) and mouse anti-β-actin (1:800, Bioworld, Nanjing, China). Bound primary antibodies were detected by HRP-conjugated goat anti-rabbit or anti-mouse antibodies. Band intensities were analyzed by densitometry scanning using Image-Pro Plus 6.0 software.

Real-time quantitative PCR analysis

The mRNA expression levels of *IFT88* and *BMPRII* after siRNA transfection for 24h were examined by qRT-PCR. Total cellular RNA was extracted using Trizol reagent (Takara Biotechnology, Dalian, China). To remove any DNA contamination, RNA samples were treated with DNase I (Invitrogen). Single stranded cDNA was synthesized from total RNA with the Primescrip™RT reagent kit (Takara Biotechnology, Dalian, China). The mRNA expression levels of the following osteogenesis-related genes and internal control *GAPDH* were analyzed by real-time PCR performed on an ABI Biosystems 7300 (Applied Biosystem, Singapore). All reactions were carried out in triplicate and expression data (after being calibrated with GAPDH levels) were analyzed using the $2^{-\triangle\triangle Ct}$ method. Optimal oligo nucleotide primers used in the above PCR assays were designed and synthesized by Takara Biotechnology based on published rat cDNA sequences: GAPDH, 5′-GGCACAGTCAAGGCTGAGAATG-3′(sense) and, 5′-ATGGTGGTGAAGACGCCAGTA-3′ (antisense); BMPRII, 5′-TGCAGATGGACGCATGGAG-3′ (sense), and 5′-GAGCCAGACGGCAAG AGCTTA-3′(antisense); IFT88, 5′-TCAGGCTATTGAGTGGCT-3′(sense), and 5′-TCTCGCAGAA CTGGGT AT-3′(antisense).

Statistical analysis

Statistical analysis was performed using SPSS 20.0 (Chicago, IL, USA). Data are reported as means ± standard deviation. Each variable was tested with n=3/group for each cell assay, and each experiment was repeated at least 3 times. ANOVA was performed with one way ANOVA followed by the Bonferroni's or LSD post hoc test. A *P*-value <0.05 was accepted as statistically significant. For graphic representation of statistical significant differences between groups, groups with * or ** are significantly different from the control or the untreated control, respectively at *P*<0.05 or 0.01. Those with & or && are different from the group treated only with PEMFs.

Results

PEMFs activated BMP-Smad1/5/8 pathway

To investigate whether BMP–Smad1/5/8 pathway was involved in the 50 Hz 0.6 mT PEMF-stimulated osteoblastic differentiation and maturation, we firstly examined the expression level of BMP2 after different time of PEMF treatment. It was found that the BMP2 protein expression was significantly

higher than the control (0 min) after 5 min (P<0.01), and peaked after 30 min. Although began to fall after 60 min and 120 min, it was still higher than the control (Figs. 1A).

Then we examined the expression levels of Smad 1/5/8, the main downstream effectors of BMP2 canonical pathway. As shown in Fig. 1A, PEMFs induced Smad1/5/8 phosphorylation rapidly and persistently. The phospho-Smad1/5/8 (p-Smad1/5/8) level was significantly higher than the control (0 min) after 5 min, and kept rising until it reached about 5 times higher than the control after 30 min, and began to decline after 60 min and 120 min, but were still higher than the control. The total protein level of Smad1/5/8 was changed in a similar tendency as with p-Smad1/5/8, but in a lesser degree.

To further identify the pathway activation, the location of p-Smad1/5/8 was examined by immunofluorescence staining and compared before and after PEMF treatment. After 30 min of PEMF treatment, p-Smad1/5/8 was positively localized in the nucleus while no nuclear translocation was found in control group (Fig. 1B). The red fluorescence intensity for nuclear p-Smad1/5/8 was more than 9 times higher in PEMFs group than in the control (P<0.01, Fig. 1C).

PEMF treatment increased the expression levels of BMPRII and BMPRIB

Since Smad1/5/8 is phosphorylated by the serine-threonine kinase of BMP receptors, we wonder whether the protein expression levels of BMP receptors were changed by PEMF treatment. As revealed by Western blot analyses shown in Fig. 1D, although PEMF treatment didn't change the expression level of BMPRIA, it significantly increased BMPRIB expression level after 15 min and 120 min (P<0.01). More obviously, PEMFs increased the expression level of BMPRII after 15 min, which was about three times higher than the control (0 min). It then began to decrease and recovered to the control level after 60 min, however, it raised to a significantly higher level again after 120 min (P<0.01).

PEMFs-induced osteogenic differentiation and mineralization was abolished by the inhibitors of BMP-Smad1/5/8 signaling

To determine whether PEMFs promoted the osteogenic differentiation and mineralization of osteoblasts through BMP-Smad1/5/8 signaling, ROBs were pretreated with 1×10^{-8} M noggin (NOG), an antagonist of BMPs [41,42], or 1×10^{-8} M LDN-193189 (LDN), an inhibitor of BMPRI kinases [43,44], and various osteogenic differentiation markers were analyzed after being treated by PEMFs. As shown in Fig. 2A, the activity of ALP, a marker enzyme for early osteogenic differentiation, was significantly

higher in the PEMF groups than in the control group after 3 days and 6 days (P<0.01), and there were no significant differences between the control and LDN or NOG alone group. However, ALP activity of PEMFs+LDN or PEMFs+NOG group were significantly decreased compared with PEMFs group (P<0.01), indicating that the promoting effect of PEMFs on ALP activity was abolished after the cells were treated by BMP signaling antagonist. The protein expression levels of Runx-2, Osx and COL-1 were also examined after 60 min of PEMF treatment. As expected, the protein expression levels of Runx-2, Osx and COL-1 in PEMFs group were significantly higher than those of the controls. However, they decreased to the control levels when LDN-193189 or noggin was added (Figs. 2B).

Formation of mineralized nodules is a representative marker for the maturation of osteoblasts. As shown in Fig. 2 C-E, PEMFs group had the largest total area (P<0.01) and highest number (P<0.01) of mineralized nodules formed from the treated osteoblasts, displaying a similar tendency with ALP activity. However, the promoting effects of PEMFs were abolished by co-treatment with LDN-193189 or noggin (P<0.01). These results confirmed that PEMFs stimulate osteoblastic differentiation and maturation by activating BMP–Smad1/5/8 signal pathway.

PEMF-induced BMP-Smad1/5/8 pathway activation needed the existence of primary cilia

To examine whether primary cilium is needed in the PEMF-induced activation of BMP-Smad1/5/8 pathway, we blocked ciliogenesis using small interfering RNA (siRNA) sequence targeting IFT88, an essential component for the assembly and maintenance of primary cilia. As a result, the mRNA and the protein expression levels of IFT88 were significantly decreased after 24 h of siRNA treatment (Fig. 3A-B). Meanwhile, as examined by immunofluorescence staining, primary cilia became dotted and obviously shorter (Fig. 3D-G), and the number of osteoblasts with primary cilia was significantly reduced (Fig. 3C).

Next, to examine the role of primary cilia in PEMF-induced BMP-Smad1/5/8 pathway activation, ROBs transfected with IFT88-targeting siRNA (siRNA) or scrambled control siRNA (Negative control, NC) were treated by 50 Hz 0.6mT PEMFs for 60min and the protein expression levels of BMP2, p-Smad1/5/8 and Smad1/5/8 were examined. As shown in Fig 4 A, while BMP2 expression level was significantly higher in the cells treated by PEMFs (PEMFs+NC group) than in NC group, it was greatly decreased in the cells transfected with IFT88-targeting siRNA and treated by PEMFs (PEMFs+siRNA group). Similarly, the increased expression level of p-Smad1/5/8 in PEMFs+NC group was markedly

decreased in PEMFs+siRNA group. PEMF treatment also induced substantial nuclear translocation of p-Smad1/5/8 in PEMFs+Nc group, however, this effect was obviously suppressed in PEMFs+siRNA group (P<0.01, Fig. 4B). This tendency was clearly shown in the quantified results of the staining intensity of p-Smad1/5/8 in the nucleus (Fig.4C). These results suggest that primary cilia are indispensable for PEMF-induced activation of BMP-Smad1/5/8 pathway.

BMPRII was localized at the base of primary cilium

With the discovery of BMPRII being the most prominently improved BMP receptor following PEMF treatment and as a step to investigate mechanisms for the role of primary cilium in the activation of BMP-Smad1/5/8 pathway, we hypothesized that the primary cilia of osteoblasts accommodate BMPRII or other signaling proteins. The distribution of BMP2, p-Smad1/5/8, Smad1/5/8 and three BMP receptors including BMPRIA, BMPIB and BMPRII were investigated by immunofluorescence staining and compared with the staining image of primary cilia. While there was no obvious overlapping staining observed between primary cilia and BMP2, p-Smad1/5/8, Smad1/5/8, BMPRIA or BMPIB, there were always dotted images of BMPRII staining that were localized at the bases of primary cilia (Fig. 5E). These differential staining patterns indicated that BMPRII localized at the bases of primary cilia should be the protein we hypothesized.

PEMF-induced increase of BMPRII expression was abolished when primary cilium was abrogated

To look for more evidence that BMPRII linking BMP-Smad1/5/8 pathway with primary cilia, we blocked ciliogenesis with siRNA interference and examined the resulting effects on BMPRII expression. As shown in Fig. 6A, while IFT88 silencing had no effect on PEMFs-induced increase of BMPRIB, it significantly blocked the increase of BMPRII expression level. Gene expression assays revealed the same tendency. The increased mRNA expression of BMPRII was significantly lower in PEMFs+siRNA group than the PEMFs+NC group (P<0.01, Fig. 6B). Besides, although BMPRII was localized to the ciliary base both in NC group and PEMFs+NC groups (Fig. 6C), no BMPRII was observed in the stunted cilia in PEMFs+siRNA group. These results indicated that the PEMF-induced increase of BMPRII expression need the existence of primary cilia, and BMPRII was the connection between the primary cilia and BMP-Smad1/5/8 pathway.

BMP2-induced BMP-Smad1/5/8 pathway activation also needed the existence of primary cilium

To investigate whether primary cilium is required for basal BMP signaling, we compared the expression levels of BMP2, BMPRII, p-Smad1/5/8 and Smad1/5/8 between the ROBs with normal primary cilia and stunted ones. As shown in Fig 7A, although the expression levels of BMP2 and Smad1/5/8 were similar between the cells with normal primary cilia and stunted ones, the expression levels of BMPRII and p-Smad1/5/8 were obviously decreased in siRNA group compared to the NC group, indicating that primary cilium is needed for keeping the basal activity of BMP signaling, and BMPRII expression is regulated by primary cilium.

To further clarify if primary cilium is required for BMP2-activated BMP signaling, we supplemented 1μg/ml BMP2 into culture media of ROBs treated with IFT88 siRNA or scrambled control siRNA and measured the expression levels of above mentioned proteins after 12 h. It was found that BMP2 significantly increased the expression levels of BMPRII and p-Smad1/5/8 in the cells of NC group (BMP2+NC group) (Fig. 7B). However, no increasing effect was observed in the cells of siRNA group (BMP2+siRNA group) and the expression levels of the two proteins were even lower than those of the NC group. These results indicated that BMP2 needs the existence of primary cilia in activating BMP signaling pathway.

Primary cilia were not affected after BMPRII expression was inhibited

Since the ciliary localization of BMPRII was disrupted when ciliogenesis is inhibited, we wonder whether ciliogenesis is affected if BMPRII expression was inhibited. We blocked BMPRII expression using the RNA interference method. As shown in Fig. 8A-B, the protein expression and mRNA expression were both significantly inhibited following siRNA treatment when compared with NC group. Then the primary cilia were observed and compared between the cells transfected with BMPRII-targeting siRNA and those transfected with scrambled control siRNA. As a result, no any difference at the cilia morphology and the fraction of cells with cilia were found (data not shown). However, the PEMF-induced osteogenic differentiation and mineralization was attenuated greatly in the cells transfected with BMPRII-targeting siRNA, which was demonstrated by the significantly decreased ALP activity after 3 days and 6 days respectively and the obviously reduced number and area of mineralized nodules formed after 12 days of osteogenic induction culture with 60 min PEMF treatment per day (Fig. 8C-E). These results indicated that although BMPRII plays an indispensable role in the PEMF-induced osteogenic

effect on osteoblasts, it has no effects on the morphology and genesis of primary cilium.

Discussion

PEMFs are a promising candidate as a natural, alternative way of preventing bone loss. As being clinically used or under clinical evaluation, it is critical to understand mechanisms of its osteogenic action. We had previously reported that 0.6 mT is an optimal intensity for 50 Hz PEMFs to stimulate osteogenic differentiation of rat calvarial osteoblasts, and this process needs the existence of primary cilia [11]. However, the detailed mechanism remains unclear. For examples, what is the molecular sensor of primary cilium in accepting PEMF signaling? How these physical stimuli are converted into intracellular signal cascades? As a ubiquitous secondary messenger and a charged molecule, the Ca^{2+} and its receptors and calcium channels have been extensively studied, and it has been found that electromagnetic fields caused an increase of calcium in many cell types [3]. Jin et al reported that flow-induced Ca^{2+} elevations occur first in the primary cilium and are followed by cytosolic Ca^{2+} mobilization [45]. Since the Ca^{2+}-permeable channel polycystin-2 (PC2) associates with the mechanosensitive protein polycystin-1 (PC-1) and localizes to the primary cilium, PC-1 has been considered a potential bone mechanosensor [46]. However, Delling et al recently reported that fluid flow did not induce calcium increase in primary cilia in many cell types including osteocyte-like cells, indicating that primary cilia are not calcium responsive mechanosensors [47]. This result challenges the traditional assumption that primary cilia sense the mechanical force through calcium-permeable ion channels within the cilia.

It has been reported that there have been several primary cilium-related pathways that play significant roles in regulating bone remodeling. Kwon et al found that primary cilia mediate the osteogenic and anti-resorptive responses of dynamic fluid flow depending on the decreases of intracellular cAMP levels and adenylyl cyclase 6 located at primary cilium [48]. Carr et al reported the human homolog of the mutated gene in the ank/ank mouse (ANKH), a widely expressed protein limiting and regulating calcification within bones, is expressed in basal body of primary cilium in the osteoblast cell line MC3T3-E1 [49]. Xiao et al shown that polycystin-1 (PC1) plays an important role in skeletogenesis through regulation of the bone-specific transcription factor Runx2-II, which co-localizes with the calcium channel polycystin-2 (PC2) in primary cilia of MC3T3-E1 osteoblasts [50]. The more recent finding that TGF-β signaling is associated with endocytosis at the pocket region of primary cilium [28] has aroused our curiosity that whether BMP-Smad1/5/8 signaling is involved in the PEMF-induced

osteogenic effects and whether this relationship is associated with the primary cilium.

As we expected, PEMF treatment indeed activated BMP-Smad1/5/8 pathway and blockage of this pathway abolished its osteogenic effect on osteoblasts. However, although we didn't find any connection between the primary cilium and signaling proteins such as BMP2, Smad1/5/8 and p-Smad1/5/8 by immunofluorescence staining method, among all BMP receptors investigated (BMPRIA, BMPRIB and BMPRII), expression levels of BMPRII were found to be readily and strongly increased by PEMF treatment, and BMPRII was localized at the base of primary cilium. When ciliogenesis was inhibited by RNA interference, the PEMF-induced increase of BMPRII expression level was also abolished, and no BMPRII could be observed any more in the inhibited primary cilia. Interestingly, although BMPRIB expression level was also increased, it was not localized at the primary cilia. It's the first time that primary cilium was found to be associated with BMP-Smad1/5/8 signaling by regulating the expression level of BMPRII which was localized at the base of primary cilia.

Our data indicated that BMPRII may have exceptional and distinctive functions, compared with BMPRI, in the activation of BMP-Smad1/5/8 signaling and osteogenic differentiation. BMPRI and BMPRII are segregated and located in aggregates with caveolae and clathrin at the surface of cells, and specific structural organization of the BMP receptors prior to BMP2 binding is a key prerequisite for activation of BMP-Smad pathways [51]. Studies have shown that stimulation with BMP2 leads to a redistribution of BMPRI and BMPRII into fewer and larger aggregates. Kinase activity of BMPRII can control the redistribution of BMPRI on the cell surface of cells, while the aggregation of BMPRII is not influenced by BMPRI. It is only influenced by the stimulation of cells with BMP2. The role of BMPRII in BMP signaling is not only to phosphorylate and activate BMPRI, but also to enhance BMP signaling [36,53].

One of the limitations of this study is that we had no means to measure the content of BMPRII in the primary cilia before and after PEMF treatment, which may provide the detailed information about the regulation mechanism of BMPRII by PEMFs. The second limitation is that we cannot tell whether there are proteins in primary cilia interacting with BMPRII to activate BMP-Smad signaling. One promising candidate is PDGFR, which plays important roles in skeletal development and bone fracture healing [54,55]. Li et al reported that PDGF-AA activates BMP-Smad1/5/8 signaling by feedback down-regulating PDGFR-α, which frees BMPRI and allows for BMPRI-BMPRII complex formation to activate smad1/5/8 [56]. Liu et al identified that PDGFR-α but not PDGFR-β participated in TGF-β1 signaling

of hepatic stellate cells. PDGFR-α knockdown inhibited TGF-β1-mediated Smad2 phosphorylation and nuclear accumulation Smad2 with no influence on noncanonical TGF-β signaling [57]. Furthermore, Schneider et al reported that the primary cilium plays a critical role in growth control via PDGFR-α which localizes to the primary cilium during growth arrest in NIH3T3 cells and primary cultures of mouse embryonic fibroblasts [15]. Clement et al found that signals initiated at the primary cilium through the PDGFR-αα cascade reorganize the cytoskeleton to regulate cell migration differentially through the AKT and the MEK1/2-ERK1/2-p90 (RSK) pathways [58]. Basing on the above reports, it is worthwhile investigating whether PEMFs activate BMP-Smad1/5/8 pathway via the interaction with PDGFRαα and BMPRII within primary cilium.

In addition, we cannot rule out the possibility that other proteins within primary cilium such as PC1 and PC2 may also take part in the pathway activation through direct or indirect interaction with BMPRII following PEMF treatment. Furthermore, apart from the BMP-Smad1/5/8 pathway, other osteogenesis-related signal pathways may also be involved in PEMF-induced osteogenic effects. Consistently, we have found that PEMF treatment increased the TCF/LEF dual-luciferase reporter activity and stimulated the increase of intracellular cAMP content (data not shown), which were related to the canonical Wnt pathway and cAMP/PKA pathway, respectively. The activation of these two pathways was either partly or indirectly regulated by primary cilium [21, 48].

In summary, the present study has found 0.6 mT 50 Hz PEMFs stimulate osteogenic differentiation and maturation of rat calvarial osteoblasts via activating BMP-Smad1/5/8 pathways. The primary cilia play an indispensable role in activating the pathway by upregulating the expression level of BMPII which was localized at the base of primary cilia. Blocking BMPRII expression was also found to significantly decrease the promoting effect of PEMFs on osteoblastic differentiation and maturation. Further studies are required to investigate the detailed mechanisms how BMPRII level is regulated by the proteins with sensing properties in primary cilia and to explore other potential pathways involved in the PEMF-induced osteogenic effects. These studies will help to screen for the optimal parameters and elucidate the mechanism of PEMFs as a noninvasive means for prevention and/or treatment of osteoporosis.

Conflict of interest

All authors have no conflicts of interest.

Acknowledgments

This work was supported by the National Natural Sciences Foundation of China (No. 81270963, 81471090 to KMC, and 81571847 to HPM) and International Science & Technology Cooperation Program of China (No. 2015DFR30940 to KMC and JFW). CJX is supported by NHMRC Australia Senior Research Fellowship (No. 1042105).

References

[1] Canalis E, Giustina A, Bilezikian JP. Mechanisms of anabolic therapies for osteoporosis. N Engl J Med 2007; 357: 905-916.

[2] Kim K, Svedbom A, Luo X, Sutradhar S, Kanis JA. Comparative cost-effectiveness of bazedoxifene and raloxifene in the treatment of postmenopausal osteoporosis in Europe, using the FRAX algorithm. Osteoporosis Int 2014; 25: 325-337.

[3] Funk RH, Monsees T, Ozkucur N. Electromagnetic effects-From cell biology to medicine. Prog Histochem Cyto 2009; 43:177-264.

[4] Jing D, Li F, Jiang M, Cai J, Wu Y, Xie K. Pulsed Electromagnetic Fields Improve Bone Microstructure and Strength in Ovariectomized Rats through a Wnt/Lrp5/β-Catenin Signaling-Associated Mechanism. Plos One 2013; 8: e79377.

[5] Li K, Ma S, Li Y, Ding G, Teng Z, Liu J, et al. Effects of PEMF exposure at different pulses on osteogenesis of MC3T3-E1 cells. Arch Oral Biol 2014; 59: 921-927.

[6] Jing D, Shen G, Huang J, Xie K, Cai J, Xu Q, et al. Circadian rhythm affects the preventive role of pulsed electromagnetic fields on ovariectomy-induced osteoporosis in rats. Bone 2009; 46: 487-495.

[7] Tabrah FL, Philip R, Mary H, Fred G. Clinical report on long-term bone density after short-term EMF application. Bioelectromagnetics 1998; 19: 75-78.

[8] Garland DE, Adkins RH, Matsuno NN, Stewart CA. The effect of pulsed electromagnetic fields on osteoporosis at the knee in individuals with spinal cord injury. J Spinal Cord Med 1999; 22: 239-245.

[9] Zhou J, Ming LG, Ge BF, Wang JQ, Zhu RQ, Wei Z, et al. Effect of 3.6-mT sinusoidal electromagnetic fields on proliferation and differentiation of osteoblasts in vitro. Bone 2012; 34: 353-358.

[10] Cheng GZ, Zhai YK, Chen KM, Zhou J, Han GQ, Zhu RQ, et al. Sinusoidal electromagnetic field stimulates rat osteoblast differentiation and maturation via activation of NO-cGMP-PKG pathway. Nitric Oxide 2011;25:316-325.

[11] Yan JL, Zhou J, Ma HP, Ma XN, Gao YH, Shi WG, et al. Pulsed electromagnetic fields promote osteoblast mineralization and maturation needing the existence of primary cilia. Mol Cell Endocrinol 2015;404:132-140.

[12] Satir P, Pedersen LB, Christensen ST. The primary cilium at a glance. J Cell Sci 2010; 123: 499-503.

[13] Espinha LC, Hoey DA, Fernandes PR, Rodrigues HC, Jacobs CR. Oscillatory fluid flow influences primary cilia and microtubule mechanics. Cytoskeleton (Hoboken) 2014;71:435-445.

[14] Chen JC, Hoey DA, Chua M, Bellon R, Jacobs CR. Mechanical signaling promote osteogenic fate through a primary cilia-mediated mechanism. FASEB J 2016;30:1504-1511.

[15] Malone AM, Anderson CT, Tummala P, Kwon RY, Johnston TR, Stearns T, et al. Primary cilia mediate mechanosensing in bone cells by a calcium-independent mechanism. Proc Natl Acad Sci USA 2007;104:13325–13330.

[16] Hoey DA, Kelly DJ, Jacobs CR. A role for the primary cilium in paracrine signaling between mechanically stimulated osteocytes and mesenchymal stem cells. Biochem Biophys Res Commun 2011;412:182–187.

[17] Temiyasathit S, Tang WJ, Leucht P, Anderson CT, Monica SD, Castillo AB, et al. Mechanosensing by the primary cilium: deletion of Kif3A reduces bone formation due to loading. PLoS ONE 2012; 7:e33368.

[18] Satir P. Primary cilia: Integral to development and disease. Dev Dynam2008; 237: 1953-1954.

[19] Schneider L, Clement CA, Teilmann SC, Pazour GJ, Hoffmann EK, Satir P, et al, PDGFR alpha signaling is regulated through the primary cilium in fibroblasts. Cur Bio 2005;15: 1861-1866.

[20] Goetz SC, Ocbina PJ, Anderson KV. The primary cilium as a Hedgehog signal transduction machine. Method Cell Biol 2009; 94:199-222.

[21] Liu B, Chen S, Helms JA. The primary cilium as an integration center for Hedgehog and Wnt signalling. Reprod Toxicol 2014; 48:19.

[22] Masyuk AI, Gradilone SA, Banales JM, Huang BQ, Masyuk TV, Lee SO, et al. Cholangiocyte primary cilia are chemosensory organelles that detect biliary nucleotides via P2Y12 purinergic receptors. Am J Physiol-Gastr L. 2008; 295: G725-G734.

[23] Christensen ST, Pedersen SF, Satir P, Veland IR, Schneider L. The Primary cilium coordinates signaling pathways in cell cycle control and migration during development and tissue repair. Curr Top Dev Biol 2008; 85:261-301.

[24] Lancaster MA, Gleeson JG. The primary cilium as a cellular signaling center: lessons from disease. Curr Opin Genet Dev 2009; 19: 220-229.

[25] Berbari NF, Lewis JS, Bishop GA, Askwith CC, Kirk M. Bardet-Biedl syndrome proteins are required for the localization of G protein-coupled receptors to primary cilia. Proc Natl Acad Sci USA 2008;105: 4242-4246.

[26] Forschbach V, Goppelt-Struebe M, Kunzelmann K, Schreiber R, Piedagnel R, Kraus A, et al. Anoctamin 6 is localized in the primary cilium of renal tubular cells and is involved in apoptosis-dependent cyst lumen formation. Cell Death Dis 2015; 6:e1899 -e1899.

[27] Rania G, Qicong H, Marion F, Marie-Christine R, Benjamin S, Serge M, et al. Septins 2, 7 and 9 and MAP4 colocalize along the axoneme in the primary cilium and control ciliary length. J Cell Sci 2013;126:2583-2594.

[28] Clement CA, Ajbro KD, Koefoed K, Vestergaard ML, Veland IR, Henriques JM, et al. TGF-β Signaling Is Associated with Endocytosis at the Pocket Region of the Primary Cilium. Cell Reports 2013; 3: 1806-1814.

[29] Hogan BL. Bone morphogenetic proteins: multifunctional regulators of vertebrate development. Gene Dev 1996;10:1580-1594.

[30] Mundy GR, Chen D, Zhao M, Dallas S, Xu C, Harris S. Growth regulatory factors and bone. Rev Endocr Metab Dis 2001; 2: 105-115.

[31] Kunikazu T, Amitabha B, Brian DH, Karen C, Sanjeev K, Louis G, et al. BMP2 activity, although dispensable for bone formation, is required for the initiation of fracture healing. Nature Genetics 2006; 38:1424-1429.

[32] Jacobs JW, Bohm M, Gupta A, Gupta SK, Wo JM. Linkage of osteoporosis to chromosome 20p12 and association to BMP2. Plos Biol 2003;1: 324-328.

[33] Lien SC, Chang SF, Lee PL, Wei SY, Chang DT, Chang JY, et al. Mechanical regulation of cancer cell apoptosis and autophagy: roles of bone morphogenetic protein receptor, Smad1/5, and p38 MAPK. Biochimica Et Biophysica Acta 2013;1833: 3124-3133.

[34] Lin GL, Hankenson KD. Integration of BMP, Wnt, and notch signaling pathways in osteoblast differentiation. J Cell Biochem 2011; 112:3491- 501.

[35] Rahman MS, Akhtar N, Jamil HM, Banik RS, Asaduzzaman SM. TGF-β/BMP signaling and other molecular events: regulation of osteoblastogenesis and bone formation. Bone Res 2015; 3:11-30.

[36] Nohe AK, Tm U, Knaus P, No P. Effect of the distribution and clustering of the type I A BMP receptor (ALK3) with the type II BMP receptor on the activation of signalling pathways. J Cell Sci, 2003;116: 3277-3284.

[37] Chen KM, Ge BF, Liu YX, Ma HP, Lu M, Bai M, Wang Y. Icariin inhibits the osteoclast formation induced by RANKL and macrophage-colony stimulating factor in mouse bone marrow culture. Die Pharmazie 2007; 62: 388-391.

[38] Clement CA, Larsen LA, Christensen ST, Using Nucleofection of siRNA Constructs for Knockdown of Primary Cilia in P19.CL6 Cancer Stem Cell Differentiation into Cardiomyocytes. Method Cell Biol 2009; 94:181-197.

[39] Bodle JC, Rubenstein CD, Phillips ME, Bernacki SH, Qi J, Banes AJ, et al. Primary Cilia: The Chemical Antenna Regulating Human Adipose- Derived Stem Cell Osteogenesis. Plos One 2013; 8: e62554-e62554.

[40] Pazour GJ, Dickert BL, Vucica Y, Seeley ES, Rosenbaum JL, Witman GB, et al. Chlamydomonas IFT88 and its mouse homologue, polycystic kidney disease gene tg737, are required for assembly of cilia and flagella. J Cell 2000; 151: 709-718.

[41] Song K, Krause CS, Patterson M, Suto R, Grgurevic L, Vukicevic S, et al. Identification of a key residue mediating bone morphogenetic protein (BMP)-6 resistance to noggin inhibition allows for engineered BMPs with superior agonist activity. J Biol Chem 2010; 285: 12169-12180.

[42] Xie ZY, Wang P, Li YX, Deng W, Zhang X, Su HJ, et al. Imbalance between BMP2 and Noggin induces abnormal osteogenic differentiation of mesenchymal stem cells in ankylosing spondylitis. Arthritis Rheumatol 2015; doi: 10.1002/art.39433.

[43] Cuny GD, Yu PB, Laha JK, Xing X, Liu JF, Lai CS, et al. Structure-activity relationship study of bone morphogenetic protein (BMP) signaling inhibitors. Bioorg Med Chem Lett. 2008;18: 4388-4392.

[44] Yu P, Lai C, Hong C, Cuny G, Bouxsein M, Hong D, et al. BMP type I receptor inhibition reduces heterotopic ossification. Nat Med 2008; 14:1363-1369.

[45] Jin X, Mohieldin AM, Muntean BS, Green JA, Shah JV, Mykytyn K, et al. Cilioplasm is a cellular compartment for calcium signaling in response to mechanical and chemical stimuli. Cell Mol Life Sci 2013;71:2165–2178.

[46] Xiao Z, Dallas M, Qiu N, Nicolella D, Cao L, Johnson M, et al. Conditional deletion of Pkd1 in osteocytes disrupts skeletal mechanosensing in mice. FASEB J 2011;25:2418-2432.

[47] Delling M, Indzhykulian AA, Liu X, Li Y, Xie T, Corey DP, et al. Primary cilia are not calcium-responsive mechanosensors. Nature 2016; 531:656-660.

[48] Kwon RY, Sara T, Padmaja T, Quah CC, Jacobs CR. Primary cilium -dependent mechanosensing is mediated by adenylyl cyclase 6 and cyclic AMP in bone cells. Faseb J 2010; 24: 2859-2868.

[49] Carr G, Moochhala SH, Eley L, Vandewalle A, Simmons NL, Sayer JA. The Pyrophosphate Transporter ANKH is Expressed in Kidney and Bone Cells and Colocalises to the Primary Cilium/Basal Body Complex. Cell Physiol Biochem 2009; 24: 595-604.

[50] Xiao Z, Zhang SB, Luo J, Quarles L. Polycystin-1 regulates skeletogenesis through stimulation of the osteoblast-specific transcription factor RUNX2-II. J Biol Chem 2008; 283: 12624-12634.

[51] Jeremy B, Adams EL, Beth B, Oleksra M, Czymmek KJ, Anja N, Initiation of BMP2 signaling in domains on the plasma membrane. J Cell Physiol 2012; 227:2880-2888.

[52] Gilboa L, Nohe A, Geissendorfer T, Sebald W, Henis YI, Knaus P. Bone morphogenetic protein receptor complexes on the surface of live cells: A new oligomerization mode for serine/threonine kinase receptors. Mol Biol Cell 2000;11: 1023-1035.

[53] Hartung A, Bitton-Worms K, Rechtman M M, et al. Different routes of bone morphogenic protein (BMP) receptor endocytosis influence BMP signaling. Mol Cell Biology, 2006, 26:7791-7805.

[54] O'Sullivan S, Naot D, Callon K, Porteous F, Horne A, Wattie D, et al. Imatinib promotes osteoblast differentiation by inhibiting PDGFR signaling and inhibits osteoclastogenesis by both direct and stromal cell-dependent mechanisms. J Bone Miner Res 2007; 22: 1679-1689.

[55] Fantauzzo KA, Soriano P, PI3K-mediated PDGFRα signaling regulates survival and proliferation in skeletal development through p53-dependent intracellular pathways. Gen Dev 2014; 28:1005-1017.

[56] Li A, Xia X, Yeh J, Kua H, Liu H, Mishina Y, et al. PDGF-AA Promotes osteogenic differentiation and migration of mesenchymal stem cell by down-regulating PDGFRα and derepressing BMP-Smad1/5/8 signaling. Plos One 2014; 9: e113785.

[57] Liu C, Li J, Xiang X, Guo L, Tu K, Liu Q, et al. PDGF receptor- promotes TGF- signaling in hepatic stellate cells via transcriptional and posttranscriptional regulation of TGF- receptors. Am J Physiol

Gastr L 2014; 307: G749-G759.

[58] Dittle LC, Sabine M, Christian S, Mette L, Peter S, Albrecht S, et al. PDGFRα signaling in the primary cilium regulates NHE1-dependent fibroblast migration via coordinated differential activity of MEK1/2-ERK1/2-p90RSK and AKT signaling pathways. J Cell Sci 2013; 126: 953-965.

Figure Legends

Fig. 1. Effect of 50Hz 0.6mT PEMF treatment on BMP-Smad1/5/8 signaling of newborn rat calvarial osteoblasts. (**A**) The protein expression levels of BMP2, p-Smad1/5/8 and Smad1/5/8 were examined by Western blotting. (**B**) The intracellular distribution of p-Smad1/5/8 was examined by immunofluorescence staining. p-Smad1/5/8 was stained by rhodamine-labeled goat anti-rabbit IgG (red), and the nucleus were stained with DAPI (blue), (bar=10μm). (**C**) The relative intensity of p-Samd1/5/8 in the nucleus was measured by Image-Pro Plus 6.0. (**D**) The protein expression levels of BMPRIA, BMPRIB and BMPRII were examined by Western blotting. $^{**}P<0.01$ *vs* control (CON).

Fig. 2. Effects of noggin (an antagonist of BMPs at 1×10^{-8} M) or LDN-193189 (an inhibitor of BMP receptor or BMPRI kinase at 1×10^{-8} M) on the PEMF-induced increase of alkaline phosphatase (ALP) activity, the expression levels of osteogenic marker proteins and mineralized nodules in ROBs. ***(A)*** ALP activities were measured after 3 days and 6 days of PEMF treatment at 60min/day. ***(B)*** The protein expression levels of COL-1, Runx-2 and Osx were examined by western blotting (standardized against β-actin) immediately after the second time of PEMF treatment. (**C**) The mineralized nodules formed after 12 days of PEMF treatment were stained by Alizarin red. (**D-E**) The areas and numbers of mineralized nodules were measured by Image-Pro Plus 6.0. $^{*}P<0.05$ or $^{**}P<0.01$ vs control (CON), $^{\&}P<0.05$ or $^{\&\&}P<0.01$ vs PEMFs group.

Fig. 3. Primary cilia of ROBs were abrogated after transfection of IFT88 siRNA. (**A**) The inhibition of IFT88 mRNA expression as revealed by real time RT-PCR, and (**B**) the protein expression inhibition as revealed by Western blotting in siRNA group compared with negative control (NC). (**B**) Percentages of cells with primary cilia in NC and siRNA groups. (D-G) Primary cilia of the NC group were stained green (green), and nuclei were stained with DAPI (blue), the primary cilia became dotted and short after 24 h of IFT88 siRNA transfection. $^{**}P<0.01$ vs NC group.

Fig. 4. The changes of BMP-2 and Smad1/5/8 protein expressions and the localization of p-Smad1/5/8 after ciliogenesis was inhibited by IFT88 siRNA in rat calvarial osteoblasts. (**A**) The protein expression levels of BMP2, Smad1/5/8 and p-Smad1/5/8 in the cells transfected with scrambled control siRNA (NC),

the cells transfected with scrambled control siRNA and treated by 50 Hz 0.6 mT PEMFs (PEMFs+NC) for 30min, and the cells transfected with IFT88 siRNA and treated by the same PEMFs (PEMFs+siRNA). (**B**) Treatment effect on p-Smad1/5/8 localization: primary cilia were stained green, p-Smad1/5/8 was stained red, and the nuclei were stained blue (with DAPI). (bar=10μm). (**C**) The relative intensity of p-Samd1/5/8 in the nucleus was measured by Image-Pro Plus 6.0. $^{**}P<0.01$ vs NC, $^{\&\&}P<0.01$ vs PEMFs+siRNA group.

Fig. 5. Effects of PEMF treatment on the localization of BMP receptors in rat calvarial osteoblasts. Primary cilia were stained green, BMPR were stained red, and nuclei were stained blue (with DAPI). bar=10μm.

Fig. 6. Effects of inhibited ciliogenesis on the protein and mRNA expressions of BMPRIB and BMPRII, and localization of BMPRII within primary cilium in rat calvarial osteoblasts. (**A**) The protein expression levels of BMPRIB and BMPRII were compared among the cells transfected with scrambled control siRNA (NC), cells transfected scrambled control siRNA and treated by 50 Hz 0.6 mT PEMFs (PEMF+NC), and the cells transfected with IFT88 siRNA and treated by the same PEMFs (PEMF+siRNA). (**B**) BMPRII mRNA expression as revealed by real time RT-PCR. (**C**) Treatment effects on BMPRII localization: primary cilia were stained green, BMPRII were stained red, and the nuclei were stained blue (with DAPI). bar=10μm. $^{**}P<0.01$ *vs* NC, $^{\&\&}P<0.01$ vs PEMFs group.

Fig. 7. Effects of IFT88 silencing on the expression levels of BMPRII, Smad1/5/8 and p-Smad1/5/8 in rat calvarial osteoblasts with or without BMP2 (1μg/mL) treatment. (**A**) The basal protein expression levels of BMPRII, p-Smad1/5/8, BMP2 and Smad1/5/8 were examined by Western blotting. (**B**) The protein expression levels of BMPRII, p-Smad1/5/8 and Smad1/5/8 were examined by Western blotting after 12 h of BMP2 treatment at 1μg/ml.

Fig. 8. Inhibition of BMPRII expression by siRNA transfection and its effect on ALP activity and mineralization of rat calvarial osteoblasts. (**A**) The gene expression of BMPRII was examined by real time RT-PCR. (**B**) The protein expression of BMPRII was examined by Western blotting. (**C**) The alkaline phosphatase (ALP) activities after 3 and 6 days of PEMF treatment in the cells transfected with

scrambled control siRNA (NC) or BMPRII siRNA and treated by PEMFs. (**D**) Mineralized nodules were stained by Alizarin red after 12 days of PEMF treatment. (**E-F**) The numbers and areas of mineralized nodules as measured by Image-Pro Plus 6.0. $^{**}P<0.01$ vs control, $^{\&\&}P<0.01$ vs PEMFs.

Fig-1

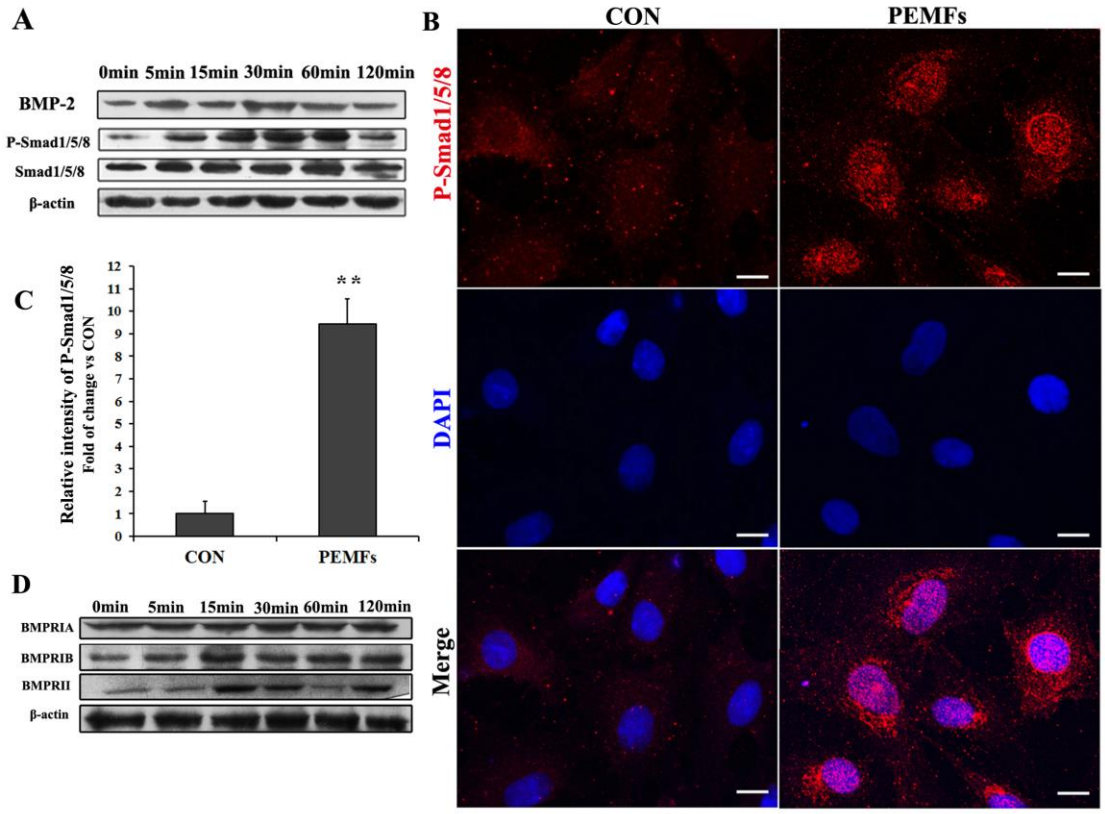


Fig-2

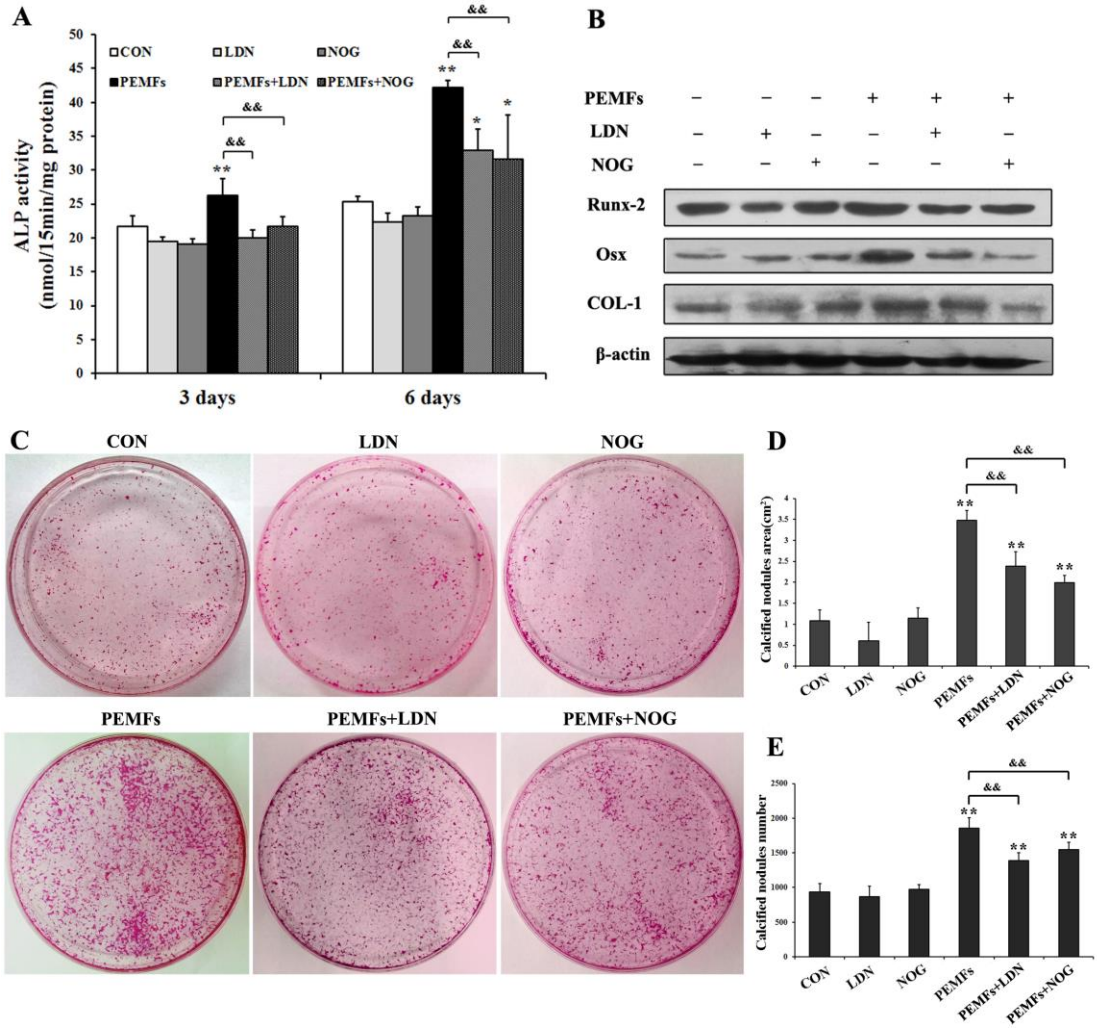

A
CON
LDN
NOG
PEMFs
PEMFs+LDN
PEMFs+NOG
ALP activity (nmol/15min/mg protein)
3 days
6 days
B
PEMFs
LDN
NOG
Runx-2
Osx
COL-1
β-actin
C
CON
LDN
NOG
PEMFs
PEMFs+LDN
PEMFs+NOG
D
Calcified nodules area(cm²)
E
Calcified nodules number

Fig-3

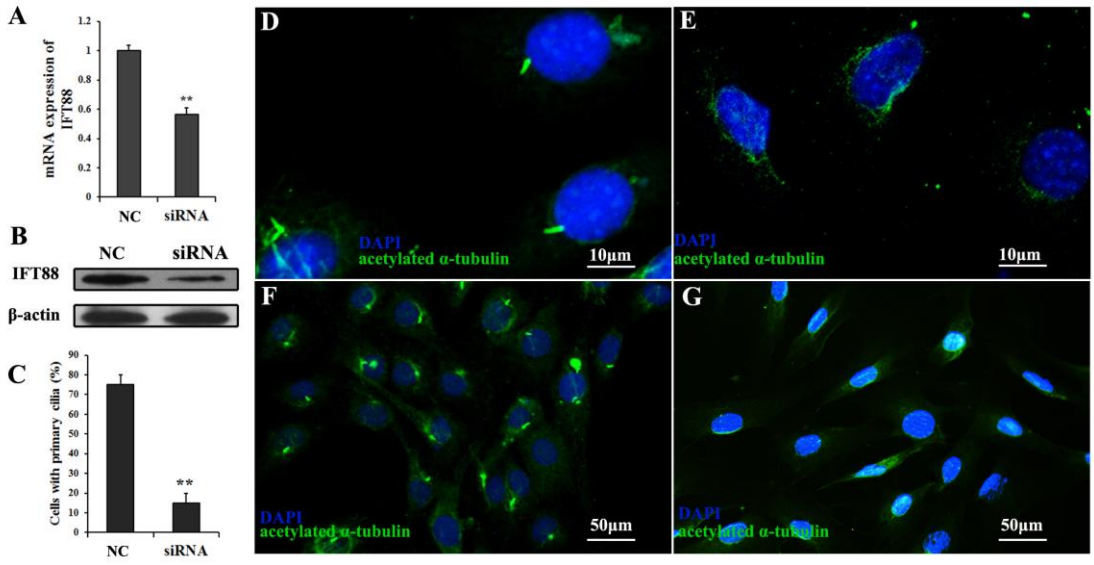

A
mRNA expression of IFT88
NC
siRNA
B
NC
siRNA
IFT88
β-actin
C
Cells with primary cilia (%)
NC
siRNA
D
DAPI
acetylated α-tubulin
10μm
E
DAPI
acetylated α-tubulin
10μm
F
DAPI
acetylated α-tubulin
50μm
G
DAPI
acetylated α-tubulin
50μm

Fig-4

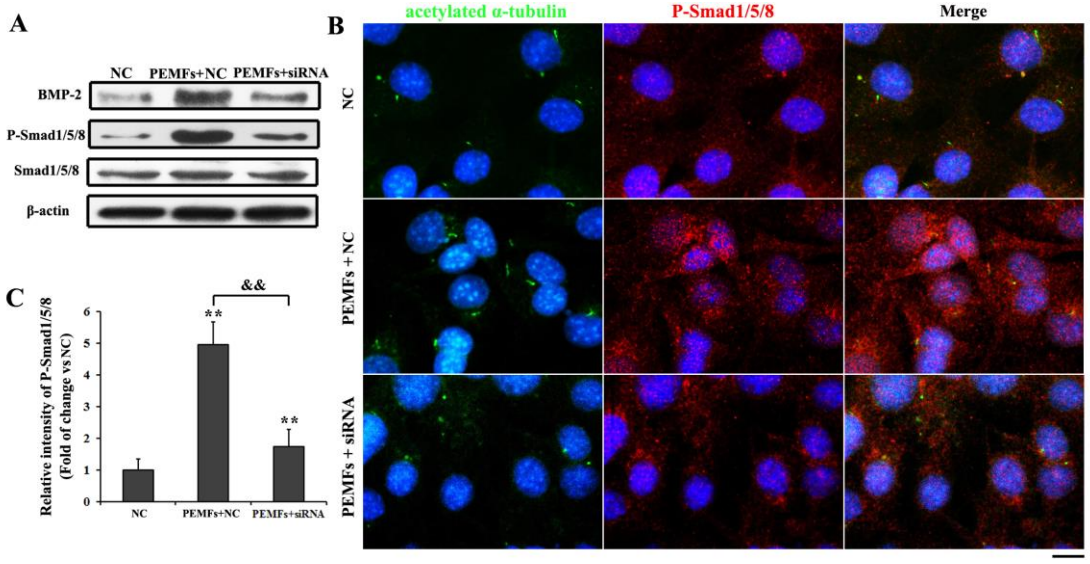

A
NC
PEMFs+NC
PEMFs+siRNA
BMP-2
P-Smad1/5/8
Smad1/5/8
β-actin
C
Relative intensity of P-Smad1/5/8 (Fold of change vs NC)
&&
NC
PEMFs+NC
PEMFs+siRNA
B
acetylated α-tubulin
P-Smad1/5/8
Merge
NC
PEMFs + NC
PEMFs + siRNA

Fig-5

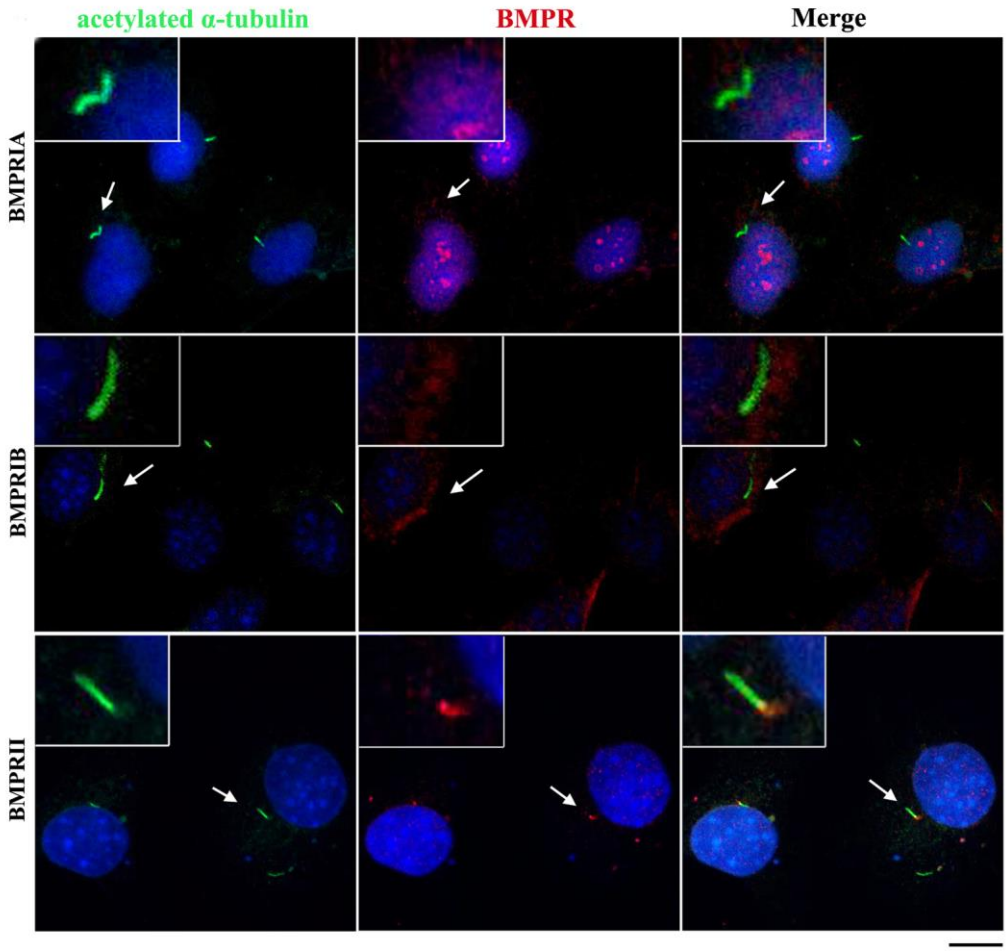

acetylated α-tubulin
BMPR
Merge
BMPRIA
BMPRIB
BMPRII

Fig-7

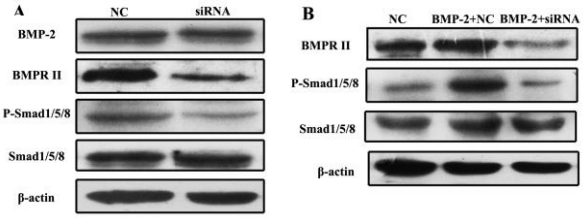
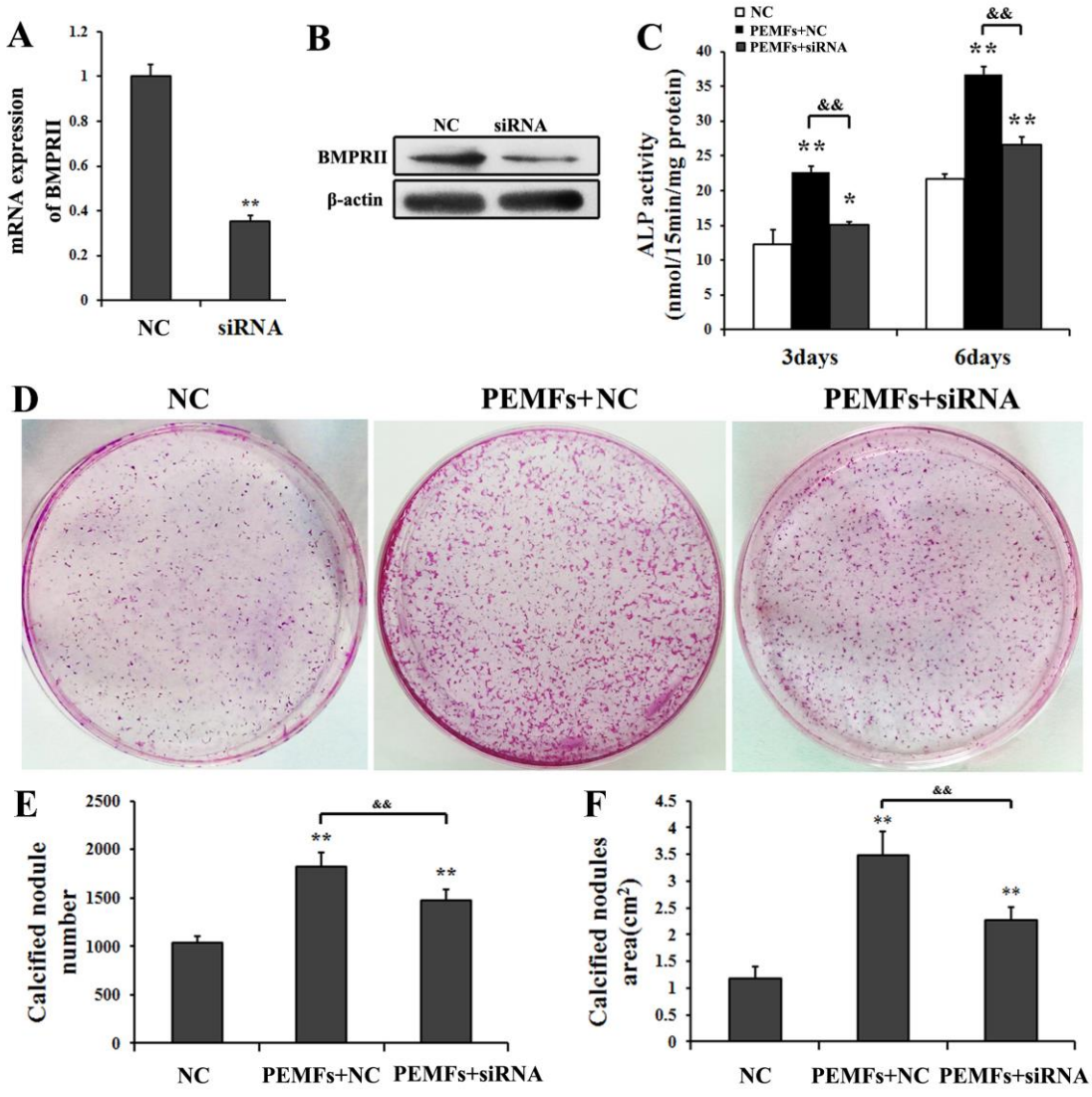

A
NC
siRNA
BMP-2
BMPR II
P-Smad1/5/8
Smad1/5/8
β-actin
B
NC
BMP-2+NC
BMP-2+siRNA
BMPR II
P-Smad1/5/8
Smad1/5/8
β-actin

Fig-8


A
mRNA expression of BMPRII
1.2
1
0.8
0.6
0.4
0.2
0
**
NC
siRNA
B
NC
siRNA
BMPRII
β-actin
C
NC
PEMFs+NC
PEMFs+siRNA
ALP activity (nmol/15min/mg protein)
40
35
30
25
20
15
10
5
0
**
*
&&
**
**
&&
3days
6days
D
NC
PEMFs+NC
PEMFs+siRNA
E
Calcified nodule number
2500
2000
1500
1000
500
0
**
**
&&
NC
PEMFs+NC
PEMFs+siRNA
F
Calcified nodules area(cm²)
4.5
4
3.5
3
2.5
2
1.5
1
0.5
0
**
**
&&
NC
PEMFs+NC
PEMFs+siRNA